PROCEEDINGS OF SCIENCE

Real-time Quantum Calculations of Phase Shifts On NISQ Hardware Platforms Using Wavepacket Time Delay

Patrick Dreher,[a,*] **Erik Gustafson,**[b] **Yingyue Zhu,**[c] **Norbert M. Linke**[c] **and Yannick Meurice**[b]

[a] *Electrical and Computer Engineering, North Carolina State University, Raleigh, NC 27695, USA*

[b] *Department of Physics and Astronomy, The University of Iowa Iowa City, IA 52242, USA*

[c] *Joint Quantum Institute and Department of Physics, University of Maryland College Park 20740, USA*

E-mail: padreher@ncsu.edu

We introduce a new method to calculate phase shifts on noisy intermediate scale quantum (NISQ) hardware platforms using a wave packet edge time delay. The method uses the early and intermediate stages of the collision because the standard method based on the asymptotic out-state behavior is unreachable using today's NISQ platforms. The calculation was implemented on a 4-site transverse Ising model in one spatial dimension with and without a potential interaction. A time evolution operator describing the progression of the system was constructed and transmission and reflection coefficients were calculated based on the identified quantum Fourier transformed momentum states. The detailed analysis of the phase shift calculations on both IBM superconducting transmon and University of Maryland ion trap quantum computers shows the platform independence of the methodology. This successful implementation of this wave packet preparation and projection on momentum eigenstates can now be performed with actual quantum computing hardware platforms. This method provides a procedure for calculating phase shifts and opens the possibility of using noisy intermediate scale quantum devices to perform real-time quantum mechanics and quantum field theory scattering calculations.

The 38th International Symposium on Lattice Field Theory, LATTICE2021 26th-30th July, 2021 Zoom/Gather@Massachusetts Institute of Technology

[*] Speaker

PoS(LATTICE2021)464

1. Introduction

Within high-energy and nuclear physics communities, there is a long term goal to develop quantum computing methods that can perform real-time evolution of an observable using the theory of strong interactions. Lattice quantum chromodynamics (QCD) is an ab-initio, ultraviolet complete formulation of this theory that has been very successful in describing the static properties of hadrons and nuclei [1] using importance sampling methods in Euclidean time. However, such lattice QCD calculations are not effective when dealing with the rapid oscillations of real-time unitary operators acting on large Hilbert spaces.

The ability to perform real-time simulations of quantum field theories would represent a major step forward in applying lattice field theory methods to physics scattering problems, ab-initio jet physics and implementation of strategies to address related question of parton distributions [2, 3]. Appplying real-time methodologies toward computations in quantum gravity [4] would also have a large potential impact.

Quantum computers offer new approaches to various sign problems and in recent years the idea of simulating quantum field theory with quantum computers has gained considerable interest [5]. However, today's noisy intermediate scale quantum (NISQ) machines are extremely limited in the size and capability to perform such computations.

An important first step toward these long-term lattice QCD goals will be to demonstrate the ability to design and implement algorithms that can model phase shifts in the scattering process that represent the total change of phase due to interactions using actual NISQ based hardware platforms. Starting from the traditional approach to quantum mechanical scattering found in standard textbooks, the phase shifts and scattering amplitudes are estimated from asymptotic data long after the collision processes have occurred. Significant progress has been made in calculating them from from finite-volume spectroscopy using lattice QCD at Euclidean time [6–11]. Because the current shortcomings of these NISQ hardware platforms have limited coherence time or gate-depth, these constraints preclude using the traditional scattering approach with the quantum computing hardware platforms.

A promising new approach to exploring scattering phase shifts with today's quantum computing hardware can be implemented if we can compute the real-time evolution "in the middle of the collision process" rather than the for asymptotic states long after the collision. For this purpose, we developed a method based on Wigner time-shift formula for the derivative of the phase shift with respect to the energy.

As a first step we implemented these ideas on the quantum Ising model (QIM). Real time evolution involving a limited number of sites for the QIM has already been attempted using a few qubits on gate based quantum computers [12–25], as well as developments in progress for more complicated models [26–40]. For processes involving a few Trotter steps, error-mitigation methods such as zero-point extrapolation [41], written for a generic noise that can be intentionally increased in order to attempt an extrapolation to zero noise, have been applied successfully [30, 42, 43]. It has been shown [15] that by modelling four qubits on an IBM Q quantum computing hardware platform these mitigation methods together with using significantly larger Trotter steps [14, 44, 45] provide

[1] See review 17 of the PDG [1].

a reasonable extrapolation for times of the order of the approximate periodicity of the problems considered.

We report that these recently developed methods can be used for state-of-the-art NISQ devices to prepare and evolve suitable wave packets for the QIM. Quantum computing algorithms are designed based on preparation of an initial state, then a real-time evolution of that state and finally a measurement of the probability for a particular final state.

In order optimize this algorithmic design under the constrained NISQ hardware resources available, we introduce the quantum Ising model with an extra interaction and its Hilbert space and focus on the reduced problem of a particle coming from the left, rebounding on a wall and returning to the left. We show that it is possible to project the wave-function in the early stages of a collision process onto momentum states and to pinpoint a time $t^\star$ corresponding to the middle of the collision with the wall. This time can be estimated by computing the time when the probability for the approximate momentum of the initial wavepacket and its opposite are equal. In practice, this can be done by introducing a normalized probability $R_-(t)$ for the reflection, defined later in Eq. (9) and which takes the value 0.5 at $t^\star$. By introducing an extra interaction close to the wall, we obtain a time delay $\Delta t^\star$ illustrated in Fig. 1. We show that $\Delta t^\star$ is half of the time delay Δt_W invoked in Wigner formula [46], provided in Eq. (6), to estimate the derivative of the phase shift with respect to the momentum.

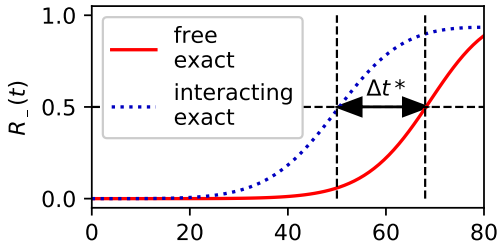

Figure 1: Illustration of the measurement of the time delay between the free and interacting wave packets. The normalized reflection probability $R_-(t)$ is defined in Eq. (9). From [47]

We can extract the phase shift by comparing the cases with and without an external potential and show that it is possible to extend the computations to the case of the quantum field theory formulations [14]. The QFT formulation requires more qubits but is guaranteed to scale efficiently for larger volumes. More specifically, it can shown [48] that for finite range interactions involving only nearest neighbor degrees of freedom, the computing time scales like the size of the system.

We have implemented this approach on both IBM superconducting transmon machines and a trapped ion system operating at the University of Maryland [49]. We present our results for the real time phase shifts measurements obtained using both hardware platforms.

2. Model for Real-time Phase shift Calculation

In this section and the next section, we follow closely Ref. [47] where we considered the transverse-field Ising model in one spatial dimension with a potential,

$$\hat{H} = -J \sum_{i=1}^{N-1} \hat{\sigma}_i^x \hat{\sigma}_{i+1}^x - h_T \sum_{i=1}^{N} \hat{\sigma}_i^z + \hat{V} \tag{1}$$

The on-site energy h_T is often called a transverse magnetic field and the ferromagnetic nearest-neighbor interaction J is responsible for particle hopping, creation and annihilation. Without $\hat{V}$, this model is very well understood [50, 51] and discussed for NISQ devices [12–15].

If we consider the case where $J \ll h_T$ the model separates into energy bands corresponding to particle number because the energy bands mix at $O(J^2)$ in perturbation theory. This significantly reduces the size of the Hilbert space and allows analytic calculations [14]. In ref. [47], a non trivial interaction which generates a phase shift (in the quantum mechanics limit), has the form

$$\hat{V} = \frac{U}{2}(1 - \hat{\sigma}^z_N). \tag{2}$$

This choice of potential allows for non-trivial scattering of a particle off of an external potential. This discrete Schrödinger equation obtained in the limit of small J, with $U = 0$, and no boundaries admits plane wave solutions $e^{\pm ikx}$ with energy

$$E(k) = 2J(1 - \cos(k)). \tag{3}$$

Imposing the boundary conditions $\psi(N + 1) = 0$ provides the following expression for the phase shift,

$$e^{i2\delta(k)} = e^{-i2k}\frac{U + Je^{ik}}{U + Je^{-ik}}, \tag{4}$$

Quantum simulations need to be carried out in finite volume. By imposing $\psi(0) = 0$, we obtain a Luscher formula

$$\delta(k) = -k(N + 1) \bmod \pi, \tag{5}$$

which introduces a restriction on the momenta. The restriction to a finite number of sites implies a N-dependence.

It was shown in [46] that

$$\Delta t_W = 2\delta'(k)/(\partial E/\partial k), \tag{6}$$

where $\partial E/\partial k$ is the group velocity, which in our case is $2J\sin(k)$. Substitution of $\delta(k)$ from Eq. (4) into Eq. (6) yields the time delay,

$$\Delta t_W = (-1 + J\frac{U\cos(k) + J}{U^2 + J^2 + 2JU\cos(k)})/J\sin(k). \tag{7}$$

In order to measure the time delay Δt_W from the first half of the scattering process, we need to measure the occupation probability in the desired momentum states $|\pm k\rangle$,

$$P_\pm(t) \equiv |\langle \pm k|\psi(t)\rangle|^2, \tag{8}$$

normalized in the following way

$$R_\pm(t) \equiv \frac{P_\pm(t)}{P_+(t) + P_-(t)} \tag{9}$$

which immediately satisfy

$$R_+ + R_- = 1. \tag{10}$$

We define the time, $t*$, when $R_+(t) = R_-(t)$. We then compare the values of t^* including and excluding the potential and call these times t^*_{free} and $t^*_{int.}$ respectively. Twice the difference between these two times is the Wigner time delay,

$$\Delta t^\star = t^*_{int.} - t^*_{free} = \frac{\Delta t_W}{2} \tag{11}$$

The details confirming these statements are elaborated in [47].

3. Explicit Calculation

The effective Hamiltonian for $N = 4$ is

$$\hat{H}_{eff} = \begin{pmatrix} 0 & -J & 0 & 0 \\ -J & 0 & -J & 0 \\ 0 & -J & 0 & -J \\ 0 & 0 & -J & U \end{pmatrix}. \tag{12}$$

This reduces effective Hamiltonian reduces the Hilbert space from 2^4 states to 4 states with the following remapping:

$$|1000\rangle \rightarrow |00\rangle,\ |0100\rangle \rightarrow |01\rangle,\ |0010\rangle \rightarrow |10\rangle,\ \text{and}\ |0001\rangle \rightarrow |11\rangle. \tag{13}$$

This is visually depicted in in Fig. 2. The Hamiltonian in Eq. (12) can now be written as

$$\hat{H}_{eff} = -J\sigma^x_{II} - \frac{J}{2}\left(\sigma^x_I\sigma^x_{II} + \sigma^y_I\sigma^y_{II}\right) + \frac{U}{4}(1-\hat{\sigma}^z_I)(1-\hat{\sigma}^z_{II}). \tag{14}$$

The subscripted roman numerals are used to indicate the use of our two-qubit decomposition.

For our simulations we set $J = 0.02$ and $U = 0.03$ and use the initial state that has some spacial localization

$$|\psi\rangle = \frac{1}{\sqrt{2}}\Big(|01\rangle + i|10\rangle\Big). \tag{15}$$

This state has significant overlap with the $k = \pi/2$ momentum state.

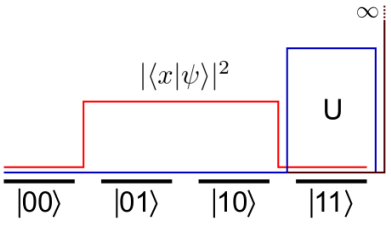

Figure 2: In this figure the qubit states rare represented by black dashes, the potential for the interacting case is in blue, the non-interacting case is in dark red, and the initial wave packet is in light red. From [47]

The following circuit constructs the wave packet with all qubits initialized in the $|0\rangle$ state.

$U_{\text{state prep}} =$ 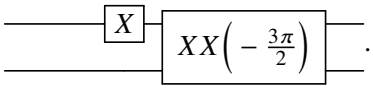

. (16)

The time evolution operator is given by

$$U_{\mathrm{Tr}}(\rho,\theta) = \tag{17}$$

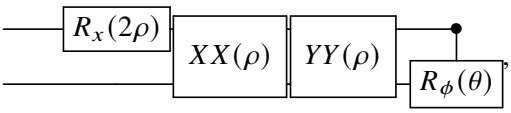

where $\rho = J\delta t$, $\theta = U\delta t$, and $\delta t = 12.5$. We use standard notations [52] for the gates,

$$XX(\rho) = e^{-i\rho XX/2},\ YY(\rho) = e^{-i\rho YY/2},\ \text{and}\ R_X(\rho) = e^{-i\rho X/2}. \tag{18}$$

The very slow growth of the one-step error for large δt [44, 45] allows us to reach $t = 75$ with only six Trotter steps [15].

A quantum Fourier transform (QFTr) on these two qubits takes this state into momentum space:

$$U_{QFTr} = \tag{19}$$

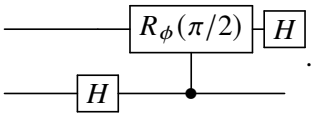

After applying the QFTr, the qubit states $|10\rangle$ and $|11\rangle$ correspond to the momentum states $|k\rangle$ and $|-k\rangle$ respectively, with $k = \pi/2$.

We fit the data to the following deformed sigmoid

$$R_{-}(t) \simeq A/(1+\exp\left(-(\frac{t-\tilde{t}^{\star}}{w})\right)), \tag{20}$$

where w describes the width of the transition region and $\tilde{t}^{\star}$ is related to $t^{\star}$ via,

$$t^{\star} = \tilde{t}^{\star} - w\,\ln(2A-1), \tag{21}$$

where w and $\tilde{t}^{*}$ are fit parameters. Due to systematic effects from the quantum computer for the interacting simulation we set A equal to the last data point, which is then excluded from the fit. For the free case, the damping occurs at later time and we set $A = 1$ and fit the standard sigmoid with the six data points.

The simulations for the full field theory follow a similar path. We prepare the initial state,

$$|\psi_i\rangle = \frac{1}{\sqrt{2}}\Big(|0100\rangle + i|0010\rangle\Big). \tag{22}$$

The Trotterization involves the natural Ising gate $e^{-iJ\delta\hat{X}\hat{X}}$ and $e^{-i\theta\hat{Z}}$. The Fourier transform can be implemented using circuit presented in [53] which can be implemented with circuit depth $O\big(n\log(n)\big)$.

The data for $R_{-}(t)$ obtained from both hardware platforms including the fits is shown in Fig 3 (left) for the effective Hamiltonian and Fig. 3 (right) for the full field theory Hamiltonian. The numerical values for Δt^{*} are provided in Table 1. The Trotter-exact and continuous-time estimates have assumed errors on par with the statistical errors from the quantum simulations,

$$\delta R_{-}(t) = \sqrt{R_{-}(t) - (R_{-}(t))^2}/\sqrt{N_{shots}}, \tag{23}$$

Type	Continuous	Trotter-exact	Trapped ions	IBM
Q.M.	-17.5(1)	-13.7(9)	-26(2)	-21(2)
Q.F.T.	-17(1)	-14.3(9)	-14(2)	-15(2)

Table 1: Results for Δt^* in the quantum mechanics limit (Q.M) and full field theory (Q.F.T.) from sigmoid fits of the simulated continuous and Trotter-exact evolutions as well as the experimental data from the trapped ions and IBM quantum computers.

with $N_{shots} = 1000$. For comparison, we give the values obtained by doing sigmoid fits of the continuous-time evolution (first column) and the Trotter steps (second column) calculated numerically at the same discrete times as the experimental data. The readout errors for the trapped ion computer were corrected by applying the state preparation and measurement correction. The readout errors were corrected on the IBM simulation using a pseudo-matrix inversion with least squares to ensure entirely physical values [54]. In addition the IBMQ Bogota simulation used Richardson extrapolations which take into account further systematic errors from the environment which produce larger uncertainties but a full extent of the systematic errors are very difficult to estimate.

We see that both the IBM and trapped ion estimates provide larger absolute values of Δt^* than the target values. This can be in part explained by the fact that the fits for the free process tend to lag below the Trotter steps for $t > 50$ indicating a loss of coherence.

Measurements from the IBMQ Bogota machine contain both the noisy data with just readout corrections and a mitigated version obtained using methods discussed in Ref. [15] and which account for some slightly negative occupations at low t. This noise mitigation involves increasing the effective error rate in the circuit by applying iterated CNOT's to increase the decoherence noise and then using a linear fit to data at different noise rates to extrapolate to a noiseless limit. The trapped ion simulations and the full field theory simulations include only readout corrections without noise mitigation due to circuit length constraints.

We see that the quantum mechanics approximation allows us to perform the QFTr and get reasonable estimates of Δt^*, (Table 1). We expect to improve the accuracy of these estimates in the near future. The extension of this procedure for more than four sites requires an all-to-all connectivity and a CNOT depth increasing with the number of sites. In contrast, the field theory calculation, which is our ultimate goal, requires more qubits but remains local [48] with a constant CNOT depth.

4. Conclusions and Next Steps

We have developed a novel method to extract the phase shift from the real-time evolution in the early stages of the scattering process. We have demonstrated that practical implementations are possible on both IBM superconducting transmon and trapped ion hardware platforms for two simulation schemes (field theory and a quantum mechanical limit). There is clearly room for optimization and at this point, we cannot claim that our results allow a systematic comparison between the two platforms.

For the next steps, we recognize that a practical implementation of the Wigner time-shift formula for the derivative of the phase shift with respect to the energy will require that we fit a

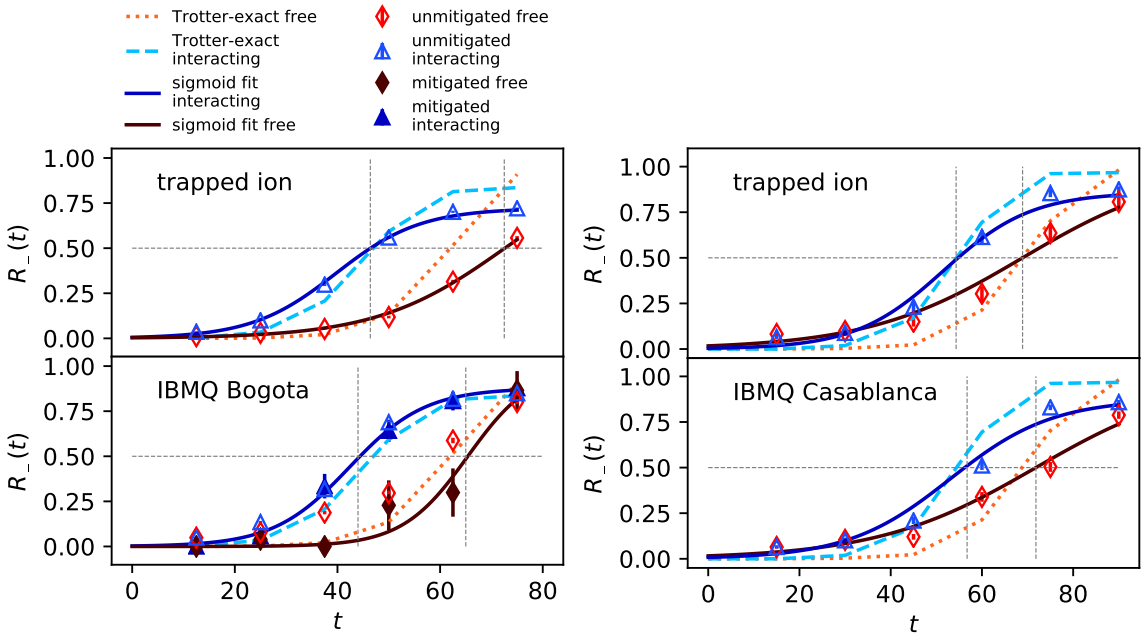

Figure 3: Figure on the left shows the quantum mechanics limit for $R_{-}(t)$. Systematic errors shown for IBM mitigated results. Figure on the right shows the experimental results for $R_{-}(t)$ using the full Hamiltonian of equation 1 with and without the interaction term. The 4 qubit trapped ion results are shown on top in figure and the IBM results in the bottom figure. The Hamiltonians use the parameters $J = 0.02$, $h_T = 1.0$, and $U = 0.03$. Statistical Errors are shown for all except for mitigated results. From [47].

normalized reflection probability with a specific model. This will capture the time delay build up in the collision process when an interaction is added. When comparing NISQ data with the model, it seemed plausible that the systematic errors relative to the signal in the early and late stage are significantly larger than the statistical errors. For future work, we plan to include reliable estimates of these systematic errors. This would allow us to sharpen the accuracy of the fits of the time shifts. We also expect that the field theory calculations should be feasible for a larger number of qubits in the near future. A detailed comparison with existing real-time methods in one spatial dimension [55–58] would be of great interest. Quantum computations for quantum Ising models in two spatial dimensions could offer the possibility to reach quantum advantage.

Acknowledgments

E. Gustafson and Y. Meurice were supported in part by the U.S. Department of Energy (DoE) under Award Number DE-SC0019139. They thank the members of QuLAT for suggestions and comments. They also thank Wayne Polyzou and the math physics seminar at the University of Iowa for fruitful discussions. P. Dreher was supported in part by the U.S. Department of Energy (DoE) under award DE-AC05-00OR22725. We thank North Carolina State University (NCSU) for access to the IBM Q Network quantum computing hardware platforms through the NCSU IBM Q Hub.

N. M. Linke acknowledges support by the DoE NP Quantum Horizons program, award number DESC0021143, and the NSF grant no. PHY-1430094 to the PFC@JQI. We are extremely grateful to Alaina M. Green, Cinthia Huerta Alderete and Nhung H. Nguyen for help with trapped-ion measurements.

References

[1] P.D. Group, P.A. Zyla et al., Review of Particle Physics, Progress of Theoretical and Experimental Physics **2020** (2020) [https://academic.oup.com/ptep/article-pdf/2020/8/083C01/34673722/ptaa104.pdf].

[2] N. Mueller, A. Tarasov and R. Venugopalan, Deeply inelastic scattering structure functions on a hybrid quantum computer, Phys. Rev. D **102** (2020) 016007.

[3] H. Lamm, S. Lawrence and Y. Yamauchi, Parton physics on a quantum computer, Physical Review Research **2** (2020) .

[4] J. Preskill, Quantum information and space-time, 2017.

[5] J. Preskill, Simulating quantum field theory with a quantum computer, in Proceedings of Science, Lattice Conference 2018, 2018, https://pos.sissa.it/334/024/pdf.

[6] M. Lüscher, Volume dependence of the energy spectrum in massive quantum field theories, Communications in Mathematical Physics **105** (1986) 153.

[7] R.A. Briceño, Z. Davoudi, T. Luu and M.J. Savage, Two-nucleon systems in a finite volume. II. ${}^3S_1 - {}^3D_1$ coupled channels and the deuteron, Phys. Rev. D **88** (2013) 114507 [1309.3556].

[8] R.A. Briceno, J.J. Dudek, R.G. Edwards and D.J. Wilson, Isoscalar $\pi\pi$ scattering and the σ meson resonance from QCD, Phys. Rev. Lett. **118** (2017) 022002 [1607.05900].

[9] R.A. Briceno, J.J. Dudek and R.D. Young, Scattering processes and resonances from lattice QCD, Rev. Mod. Phys. **90** (2018) 025001 [1706.06223].

[10] M.J. Savage, Nuclear Physics, PoS **LATTICE2016** (2016) 021 [1611.02078].

[11] Z. Davoudi, The path from finite to infinite volume: Hadronic observables from lattice QCD, PoS **LATTICE2018** (2018) 014 [1812.11899].

[12] A. Cervera-Lierta, Exact Ising model simulation on a quantum computer, Quantum **2** (2018) 114.

[13] H. Lamm and S. Lawrence, Simulation of Nonequilibrium Dynamics on a Quantum Computer, Phys. Rev. Lett. **121** (2018) 170501 [1806.06649].

[14] E. Gustafson, Y. Meurice and J. Unmuth-Yockey, Quantum simulation of scattering in the quantum ising model, Physical Review D **99** (2019) .

[15] E. Gustafson, P. Dreher, Z. Hang and Y. Meurice, Indexed improvements for real-time trotter evolution of a (1 + 1) field theory using NISQ quantum computers, Quantum Science and Technology **6** (2021) 045020.

[16] M. Kim, Y. Song, J. Kim and J. Ahn, Quantum ising hamiltonian programming in trio, quartet, and sextet qubit systems, PRX Quantum **1** (2020) .

[17] K. Yeter-Aydeniz, G. Siopsis and R.C. Pooser, Scattering in the ising model using quantum lanczos algorithm, 2021.

[18] J. Vovrosh and J. Knolle, Confinement and entanglement dynamics on a digital quantum computer, 2001.03044.

[19] Y. Salathé, M. Mondal, M. Oppliger, J. Heinsoo, P. Kurpiers, A. Potočnik et al., Digital quantum simulation of spin models with circuit quantum electrodynamics, Physical Review X **5** (2015) .

[20] W.L. Tan, P. Becker, F. Liu, G. Pagano, K.S. Collins, A. De et al., Domain-wall confinement and dynamics in a quantum simulator, Nature Physics (2021) .

[21] A. Smith, M.S. Kim, F. Pollmann and J. Knolle, Simulating quantum many-body dynamics on a current digital quantum computer, npj Quantum Information **5** (2019) .

[22] H. Labuhn, D. Barredo, S. Ravets, S. de Léséleuc, T. Macrì, T. Lahaye et al., Tunable two-dimensional arrays of single rydberg atoms for realizing quantum ising models, Nature **534** (2016) 667–670.

[23] J. Zhang, G. Pagano, P.W. Hess, A. Kyprianidis, P. Becker, H. Kaplan et al., Observation of a many-body dynamical phase transition with a 53-qubit quantum simulator, **551** (2017) 601 [1708.01044].

[24] T. Kadowaki and H. Nishimori, Quantum annealing in the transverse ising model, Phys. Rev. E **58** (1998) 5355.

[25] H. Bernien, S. Schwartz, A. Keesling, H. Levine, A. Omran, H. Pichler et al., Probing many-body dynamics on a 51-atom quantum simulator, **551** (2017) 579 [1707.04344].

[26] A. Alexandru, P.F. Bedaque, S. Harmalkar, H. Lamm, S. Lawrence and N.C. Warrington, Gluon field digitization for quantum computers, Physical Review D **100** (2019) .

[27] E. Zohar, J.I. Cirac and B. Reznik, Quantum simulations of gauge theories with ultracold atoms: Local gauge invariance from angular-momentum conservation, Physical Review A **88** (2013) .

[28] E.A. Martinez, C.A. Muschik, P. Schindler, D. Nigg, A. Erhard, M. Heyl et al., Real-time dynamics of lattice gauge theories with a few-qubit quantum computer, Nature **534** (2016) 516–519.

[29] B. Buyens, J. Haegeman, F. Hebenstreit, F. Verstraete and K. Van Acoleyen, Real-time simulation of the Schwinger effect with Matrix Product States, Phys. Rev. D **96** (2017) 114501 [1612.00739].

[30] N. Klco, E.F. Dumitrescu, A.J. McCaskey, T.D. Morris, R.C. Pooser, M. Sanz et al., Quantum-classical computation of Schwinger model dynamics using quantum computers, Phys. Rev. **A98** (2018) 032331 [1803.03326].

[31] R.C. Brower, D. Berenstein and H. Kawai, Lattice gauge theory for a quantum computer, 2020.

[32] P.I. Karpov, G.Y. Zhu, M.P. Heller and M. Heyl, Spatiotemporal dynamics of particle collisions in quantum spin chains, 2011.11624.

[33] E.T. Holland, K.A. Wendt, K. Kravvaris, X. Wu, W.E. Ormand, J.L. DuBois et al., Optimal control for the quantum simulation of nuclear dynamics, Physical Review A **101** (2020) .

[34] A. Roggero, C. Gu, A. Baroni and T. Papenbrock, Preparation of excited states for nuclear dynamics on a quantum computer, Physical Review C **102** (2020) .

[35] F.M. Surace and A. Lerose, Scattering of mesons in quantum simulators, 2011.10583.

[36] D.E. Kharzeev and Y. Kikuchi, Real-time chiral dynamics from a digital quantum simulation, Phys. Rev. Res. **2** (2020) 023342 [2001.00698].

[37] K. Ikeda, D.E. Kharzeev and Y. Kikuchi, Real-time dynamics of Chern-Simons fluctuations near a critical point, 2012.02926.

[38] R.A. Briceño, J.V. Guerrero, M.T. Hansen and A. Sturzu, The role of boundary conditions in quantum computations of scattering observables, 2007.01155.

[39] M. Van Damme, L. Vanderstraeten, J. De Nardis, J. Haegeman and F. Verstraete, Real-time scattering of interacting quasiparticles in quantum spin chains, Phys. Rev. Research **3** (2021) 013078.

[40] M.C. Bañuls et al., Simulating Lattice Gauge Theories within Quantum Technologies, Eur. Phys. J. D **74** (2020) 165 [1911.00003].

[41] L.F. Richardson and J.A. Gaunt, Viii. the deferred approach to the limit, Philosophical Transactions of the Royal Society A: Mathematical, Physical and Engineering Sciences **226** (1927) .

[42] A. Kandala, K. Temme, A.D. Córcoles, A. Mezzacapo, J.M. Chow and J.M. Gambetta, Error mitigation extends the computational reach of a noisy quantum processor, Nature **567** (2019) 491–495.

[43] A. Kandala, A. Mezzacapo, K. Temme, M. Takita, M. Brink, J.M. Chow et al., Hardware-efficient variational quantum eigensolver for small molecules and quantum magnets, Nature **549** (2017) 242 EP .

[44] Y. Meurice, Quantum field theory: a quantum computation approach, Institute of Physics Publishing, Bristol (2021).

[45] Y. Meurice, R. Sakai and J. Unmuth-Yockey, Tensor field theory with applications to quantum computing, 2010.06539.

[46] E.P. Wigner, Lower limit for the energy derivative of the scattering phase shift, Phys. Rev. **98** (1955) 145.

[47] E. Gustafson, Y. Zhu, P. Dreher, N.M. Linke and Y. Meurice, Real-time quantum calculations of phase shifts using wave packet time delays, Physical Review D **104** (2021) .

[48] S. Lloyd, Universal quantum simulators, Science **273** (1996) 1073.

[49] S. Debnath, N.M. Linke, C. Figgatt, K.A. Landsman, K. Wright and C. Monroe, Demonstration of a small programmable quantum computer with atomic qubits, Nature **536** (2016) 63.

[50] J.B. Kogut, An introduction to lattice gauge theory and spin systems, Rev. Mod. Phys. **51** (1979) 659.

[51] J.B. Kogut, The lattice gauge theory approach to quantum chromodynamics, Rev. Mod. Phys. **55** (1983) 775.

[52] M. Nielsen and I. Chuang, Quantum Computation and Quantum Information, Cambridge Series on Information and the Natural Sciences, Cambridge University Press (2000).

[53] A.J. Ferris, Fourier transform for fermionic systems and the spectral tensor network, Phys. Rev. Lett. **113** (2014) 010401.

[54] I. Research and the IBM QX team, IBM Q Experience User Guide. https://qiskit.github.io/ibmqx-user-guides/full-user-guide/introduction.html, 2017.

[55] G. Vidal, Efficient simulation of one-dimensional quantum many-body systems, Phys. Rev. Lett. **93** (2004) 040502.

[56] S.R. White and A.E. Feiguin, Real-time evolution using the density matrix renormalization group, Phys. Rev. Lett. **93** (2004) 076401.

[57] F. Verstraete, J.J. García-Ripoll and J.I. Cirac, Matrix product density operators: Simulation of finite-temperature and dissipative systems, Phys. Rev. Lett. **93** (2004) 207204.

[58] A.J. Daley, C. Kollath, U. Schollwöck and G. Vidal,
Time-dependent density-matrix renormalization-group using adaptive effective Hilbert spaces,
Journal of Statistical Mechanics: Theory and Experiment **2004** (2004) 04005
[cond-mat/0403313].